Chinese Physics Letters

LETTER

# Pressure-Driven Electronic Reconstruction and Anomalous Hall Transport Evolution in Monoclinic $FeNbTe_2$

Cite as: Pengyu Su *et al*. 2026 *Chin. Phys. Lett.* **43** 070705

DOI CSTR

## Recommended Articles

**Pressure-Enhanced Intrinsic Anomalous Hall Conductivity in the Kagome Ferrimagnet $TbMn_6Sn_6$**

Hao Sun *et al*.
*Chin. Phys. Lett.* **43**, 030704 (2026)

**Pressure-Tunable Large Anomalous Hall Effect in Ferromagnetic Metal $LiMn_6Sn_6$**

Lingling Gao *et al*.
*Chin. Phys. Lett.* **41**, (2024)

**Pressure-Tuned Intrinsic Anomalous Hall Conductivity in Kagome Magnets $RV_6Sn_6$ ($R$ = Gd, Tb)**

Xiangming Kong *et al*.
*Chin. Phys. Lett.* **41**, (2024)

**Symmetry-Constrained Anomalous Transport in the Altermagnetic Material $CuX_2$ (X = F, Cl)**

Zhengxuan Wang, Ruqian Wu, Chunlan Ma, Shijing Gong, Chuanxi Zhao, Shuaikang Zhang, Guangtao Wang, Tianxing Wang, and Yipeng An
*Chin. Phys. Lett.* **42**, 080705 (2025)

**Giant Anomalous Nernst Angle Induced by Berry Curvature in Layered Itinerant Ferromagnets**

Yu-Ting Qian, Jiu-Yun Zhang, Xiang-Yu Bi, Peng Chen, Hong-Zi Cao, Wei-Feng Xu, Zhong-Yuan Liu, Kun Zhai, Hong-Tao Yuan, and Jun-Wei Huang
*Chin. Phys. Lett.* **42**, 090713 (2025)

**Large Anomalous Hall Conductivity in Quasi-One-Dimensional Geometrically Frustrated Metal $Pr_3MnBi_5$**

Xinyao Li, Feihong Guan, Xinhang Shan, Xiangde Zhu, Wei Ning, and Mingliang Tian
*Chin. Phys. Lett.* **43**, 040702 (2026)

A series journal of Chinese Physical Society distributed by IOP Publishing

Chinese Physics Letters

*Chin. Phys. Lett.* **43** 070705 (2026)

LETTER

DOI: 10.1088/0256-307X/43/7/070705
CSTR: 32039.14.0256-307X.43.7.070705

# Pressure-Driven Electronic Reconstruction and Anomalous Hall Transport Evolution in Monoclinic $FeNbTe_2$

**Pengyu Su(苏鹏宇)[1,†], Zhaoyu Zhu(朱昭宇)[2,†], Jingyi He(何景艺)[3], Jing Wang(王晶)[4], Weiwei Wang(王伟玮)[5], Chenchao Xu(徐陈超)[2,*], Haiyang Yang(杨海洋)[1,*], and Jie Wu(吴颉)[3,*]**

[1]College of Materials and Environmental Engineering, Hangzhou Dianzi University, Hangzhou 310018, China
[2]School of Physics, Hangzhou Normal University, Hangzhou 311121, China
[3]Department of Physics, School of Science, Westlake University, Hangzhou 310024, China
[4]State Key Laboratory of Surface Physics, Department of Physics, Fudan University, Shanghai 200438, China
[5]Shanghai Synchrotron Radiation Facility, Shanghai Advanced Research Institute, Chinese Academy of Sciences, Shanghai 201204, China

[†]These authors contributed equally to this work.
[*]Corresponding authors. Email: chenchao-xu@hznu.edu.cn; hyyang@hdu.edu.cn; wujie@westlake.edu.cn

**Pressure provides a clean route to uncover hidden electronic and magnetic instabilities in layered tellurides by continuously tuning bandwidths and Fermi-surface topology without introducing chemical disorder. Here we report high-pressure electrical transport, magnetoresistance, Hall effect, and synchrotron x-ray diffraction measurements on single-crystalline monoclinic $FeNbTe_2$. At ambient pressure, $FeNbTe_2$ displays a low-temperature resistive upturn together with negative magnetoresistance and an anomalous Hall effect. Upon compression across $P_c \sim 5.5$ GPa, the resistive upturn is fully suppressed, the anomalous Hall response collapses, and the Hall coefficient reverses sign. Room-temperature high-pressure synchrotron x-ray diffraction reveals that the monoclinic structure remains stable throughout the investigated pressure range, with no evidence for a symmetry-changing structural transition. These combined results suggest a pressure-driven electronic reconstruction near $P_c$ within the preserved monoclinic framework, accompanied by a marked modification of the magnetic transport response. Our work establishes monoclinic $FeNbTe_2$ as a useful platform for exploring pressure-controlled electronic reconstruction and anomalous transverse transport in layered magnetic tellurides.**

## Introduction

The anomalous Hall effect (AHE) is a particularly sensitive transverse transport response to changes in electronic structure in magnetic solids. In systems with broken time-reversal symmetry, the Hall signal generally contains an ordinary contribution associated with the Lorentz force and an anomalous contribution arising from either extrinsic scattering or intrinsic Berry-curvature effects [1,2]. Because the AHE depends not only on magnetic order but also on the low-energy electronic states near the Fermi level, it has become an effective probe of how carrier dynamics, scattering channels, and band topology evolve under external tuning [3–8]. Among the available tuning parameters, pressure is especially powerful because it continuously modifies interatomic distances, bandwidths, and Fermi-surface geometry without introducing chemical disorder [9–13].

Recent high-pressure studies have shown that the AHE can respond to compression in strikingly different ways depending on the material. In GdPtBi, pressure continuously suppresses the anomalous Hall conductivity even though Weyl-related signatures remain, underscoring the sensitivity of the transverse response to the Fermi-level position and spin configuration [14]. In $CsV_3Sb_5$, pressure drives a sign reversal of the anomalous Hall signal, likely through a reconstruction of the pressure-modified electronic structure [15]. In $CrGeTe_3$, the AHE emerges only after the system becomes metallic and then evolves nonmonotonically with further compression [16]. These examples highlight pressure as an effective means of disentangling the intertwined roles of electronic structure, carrier balance, and ordered states in shaping anomalous transverse transport.

Against this background, $FeNbTe_2$ provides an appealing platform because its magnetic and transport properties vary across different structural polymorphs. Earlier work on the orthorhombic phase revealed antiferromagnetic correlations, spin-glass-like behavior, and unsaturated negative magnetoresistance [17–21]. By contrast, a recently identified monoclinic polymorph exhibits long-range ferromagnetic order together with an anomalous Hall response [22–24]. Since these polymorphs retain the same layered Nb–Te framework but differ in the local symmetry around Nb [22], monoclinic $FeNbTe_2$ offers a valuable opportunity to examine how compression tunes the interplay among crystal structure, magnetic order, and transverse transport in a layered telluride.

In this work, we investigate the pressure evolution of single-crystalline monoclinic $FeNbTe_2$ by combining electrical transport, magnetoresistance, Hall effect, and synchrotron x-ray diffraction (XRD) measurements. We show that a pronounced set of transport anomalies develops near a characteristic pressure $P_c \sim 5.5$ GPa, where the low-temperature transport changes abruptly, the anomalous Hall and magnetoresistance responses are rapidly suppressed, and the Hall coefficient reverses sign. Meanwhile, room-temperature high-pressure XRD shows that the monoclinic structure remains stable up to at least 18.1 GPa, with no evidence for a conventional symmetry-changing structural phase transition, although a subtle anomaly in the $a/c$ ratio is detected near the same pressure.

## Results and Discussion

The detailed experimental and computational methods and supporting data are available in the Supplemental Material (SM) [25–36]. $FeNbTe_2$ crystallizes in a monoclinic structure with space group $P2_1/c$ (No. 14). As shown in Fig. 1(a), the crystal consists of layered units stacked along the crystallographic $a$ axis, with Nb and Fe atoms sandwiched between Te layers. Within each layer, Nb forms distorted $NbTe_6$ octahedra, while Fe occupies interstitial sites and forms $FeTe_4$ tetrahedra. Neighboring Fe atoms further form dumbbell-like motifs

Received 12 April 2026; accepted 12 June 2026; published 7 July 2026
© 2026 Chinese Physical Society and IOP Publishing Ltd. All rights, including for text and data mining, AI training, and similar technologies, are reserved.

Check for updates

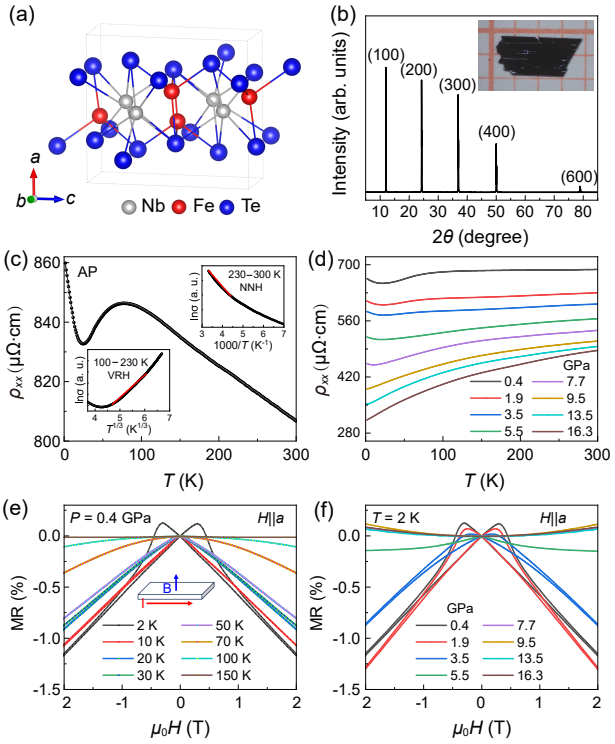


**Fig. 1.** (a) Crystal structure of monoclinic $FeNbTe_2$. The dashed rectangle marks the unit cell. (b) Room-temperature XRD pattern measured on the natural cleavage plane of $FeNbTe_2$ single crystal. Only ($h$00) reflections are observed. Inset: photograph of as-grown $FeNbTe_2$ single crystal. (c) Temperature dependence of the longitudinal resistivity $\rho_{xx}$ ($T$) at ambient pressure. Left inset: ln$\sigma$ plotted as a function of $T^{1/3}$ in the range 100–230 K. Right inset: ln$\sigma$ plotted as a function of 1000/$T$ in the range 230–300 K. (d) Temperature dependence of $\rho_{xx}$ ($T$) under pressures from 0.4 to 16.3 GPa. (e) Magnetoresistance (MR) measured at various temperatures under 0.4 GPa with magnetic field applied parallel to the $a$-axis. (f) Field dependence of the MR at 2 K under various pressures for $H \parallel a$.

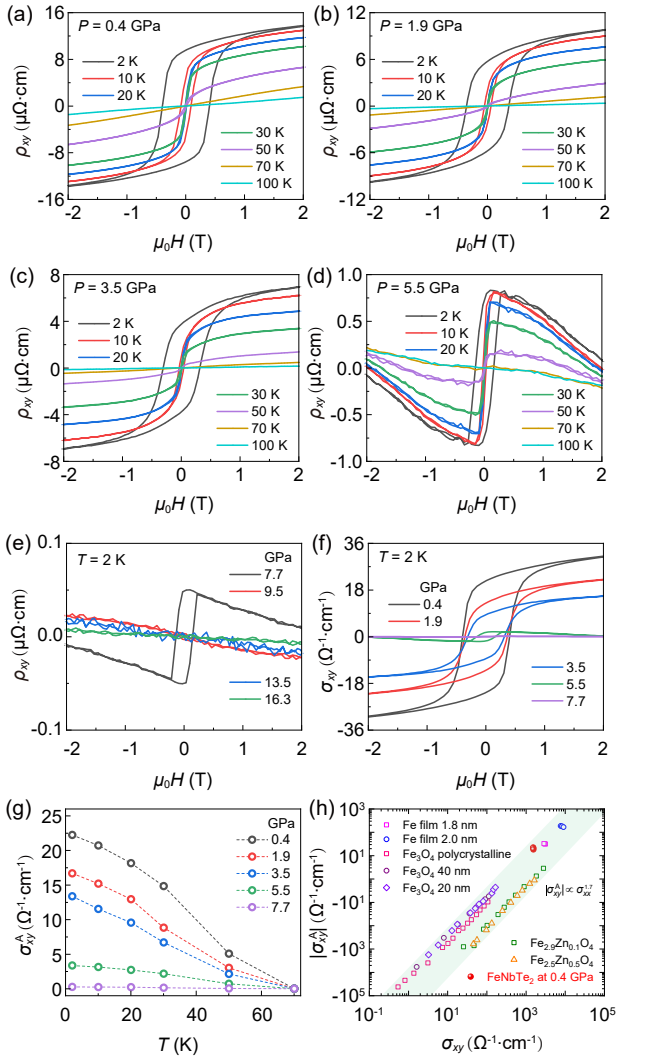


**Fig. 2.** Field dependence of the Hall resistivity $\rho_{xy}(H)$ measured at selected temperatures under pressures of (a) 0.4, (b) 1.9, (c) 3.5, and (d) 5.5 GPa. (e) $\rho_{xy}(H)$ measured at 2 K under higher pressures of 7.7, 9.5, 13.5, and 16.3 GPa. The anomalous Hall resistivity $\rho_{xy}^{A}$ is characterized by the zero-field remanent Hall signal of the hysteresis loop. (f) Field dependence of the anomalous Hall conductivity $\sigma_{xy}^{A}$ at 2 K under different pressures. (g) Temperature dependence of $\sigma_{xy}^{A}$ under different pressures. (h) Log-log plot of the absolute anomalous Hall conductivity $|\sigma_{xy}^{A}|$ as a function of the longitudinal conductivity $\sigma_{xx}$ for $FeNbTe_2$ at 0.4 GPa. Data for representative ferromagnets are taken from Ref. [1]. The shaded region marks the bad-metal regime characterized by the empirical scaling relation $|\sigma_{xy}^{A}| \propto \sigma_{xx}^{1.7}$.

mediated by Te atoms, giving rise to a quasi-two-dimensional framework [17]. Room-temperature XRD shows only ($h$00) reflections [Fig. 1(b)], confirming that the natural cleavage plane is parallel to the $bc$ plane and that the as-grown single crystals are of high quality. The temperature dependence of the longitudinal resistivity at ambient pressure is shown in Fig. 1(c). Upon warming from 1.8 K, first decreases to a minimum near 25 K, then increases to a broad maximum around 75 K, and finally decreases gradually toward room temperature. This nonmonotonic behavior is consistent with earlier reports on monoclinic $FeNbTe_2$ [24], where the low-temperature transport was discussed in terms of hopping-like conduction together with magnetic scattering [37,38]. The inset analysis likewise suggests that different transport channels dominate in different temperature windows.

Having established the ambient-pressure transport background, we now turn to its evolution under compression. As shown in Fig. 1(d), the resistivity changes markedly with increasing pressure. At 0.4 GPa, the high-temperature part of $\rho_{xx}(T)$ already shows metallic behavior, although a weak low-temperature upturn remains below about 25 K. This upturn persists up to 5.5 GPa, but is rapidly suppressed above 7.7 GPa, where the broad feature near 75 K also disappears. With further compression, $FeNbTe_2$ exhibits metallic behavior over the entire measured temperature range, and no superconductivity is observed down to 1.8 K. Such pressure-induced metallization is phenomenologically reminiscent of the recent high-pressure behavior reported for the kagome ferromagnet CrNiAs [39], where metallic transport reappears as the magnetic transitions are suppressed and the anomalous Hall signal is gradually reduced. A similar evolution is seen in the magnetoresistance. At 0.4 GPa, the MR measured with $H \parallel a$ exhibits a butterfly-shaped hysteresis loop at 2 K [Fig. 1(e)], consistent with the ferromagnetic state reported previously [22,24]. Its magnitude decreases with increasing temperature and becomes nearly negligible above $T_c$. As summarized in Fig. 1(f), the hysteretic negative MR changes little up to 3.5 GPa, but is strongly suppressed at 5.5 GPa and becomes positive by 7.7 GPa. This crossover from negative MR to positive MR suggests that the transport signatures associated with ferromagnetic scattering are rapidly weakened under pressure, while the ordinary orbital MR contribution becomes increasingly important.

To further track the pressure evolution of the transverse response, we next examine the Hall effect. As shown in Figs. 2(a)–2(e), the Hall resistivity $\rho_{xy}(H)$ at low pressures consists of a pronounced low-field hysteresis superimposed on an approximately linear high-field background. The low-field hysteresis reflects the anomalous Hall effect associated with the ferromagnetic state. Since the ordinary Hall term vanishes at zero field, the zero-field remanent Hall signal of the hysteresis loop is used to characterize $\rho_{xy}^{A}$. From 0.4 to 3.5 GPa, the high-field slope remains positive and the anomalous Hall signal is still

sizable, indicating that the low-pressure state is largely preserved in this range. With further compression, however, the Hall response changes abruptly. At 5.5 GPa, the anomalous Hall resistivity is rapidly reduced and the coercive field becomes much smaller. At the same time, the high-field slope of $\rho_{xy}(H)$ reverses sign, pointing to a substantial reorganization of the dominant carrier contribution. A two-band analysis at 70 K suggests that the Hall-sign reversal is accompanied by an enhanced electron-like contribution and a suppressed hole-like contribution across $P_c \sim 5.5$ GPa (see Section S2 of the SM). By 7.7 GPa, the anomalous Hall component is nearly suppressed, and no clear hysteresis can be resolved at still higher pressures.

The same pressure evolution is reflected more directly in the anomalous Hall conductivity $\sigma_{xy}^{A}$, shown in Figs. 2(f) and 2(g). At 2 K and 0.4 GPa, $\sigma_{xy}^{A}$ reaches about 24 $\Omega^{-1}\cdot cm^{-1}$, but decreases rapidly with increasing pressure and becomes nearly negligible above 5.5 GPa. To gain further insight into the origin of the AHE, we first compare our data with the empirical scaling behavior reported for ferromagnets in different transport regimes [1]. As shown in Fig. 2(h), the $FeNbTe_2$ data point at 0.4 GPa falls in the bad-metal–hopping regime of the anomalous Hall phase diagram. Together with the hopping-like low-temperature transport observed at ambient pressure [24], this suggests that the AHE in $FeNbTe_2$ develops in a disorder-sensitive bad-metal–hopping regime, where scattering-related contributions are expected to be important. Since this empirical comparison alone cannot uniquely determine the AHE mechanism, we further calculated the intrinsic anomalous Hall conductivity from the Berry curvature of the electronic bands under pressure (see Section S3 of the SM). At the calculated Fermi level, the clean-limit intrinsic AHC increases with compression, which is opposite to the experimental trend of the rapidly suppressed. This contrast indicates that the pressure evolution of the measured AHE cannot be understood in terms of the intrinsic Berry-curvature contribution alone. Instead, the observed AHE is more likely governed by scattering-related extrinsic contributions in the bad-metal–hopping regime. The rapid suppression of, together with the occurrence of positive MR and the sign reversal of the ordinary Hall coefficient, further points to a substantial modification of the scattering-related magnetic transport response under pressure.

The remaining question is whether these transport anomalies are accompanied by a crystallographic instability. Room-temperature high-pressure synchrotron XRD [Fig. 3(a)] shows that all diffraction peaks shift systematically toward higher angles with increasing pressure, while no additional reflections appear throughout the measured range. Le Bail refinements further show that all patterns can be consistently indexed within the monoclinic $P2_1/c$ structure, indicating that the lattice symmetry remains unchanged under compression. The pressure dependences of the lattice parameters and unit-cell volume are summarized in Figs. 3(b) and 3(c). The volume–pressure relation is well described by a Birch–Murnaghan equation of state [40], yielding a bulk modulus $B_0 = 51.7$ GPa. At the same time, a weak anomaly is observed near 6 GPa in the compression behavior of the lattice parameter $a$, which corresponds to the stacking direction of the layered units.

Taken together, the transport results identify a characteristic pressure $P_c \sim 5.5$ GPa in monoclinic $FeNbTe_2$, across which the electronic transport and anomalous magnetic transport response change markedly (Fig. 4). We note that different pressure-transmitting media were used for transport and XRD measurements, and their possible influence is discussed in Section S4 of the SM. The weak anomaly in $a/c$ may provide a structural clue to the pressure-induced electronic evolution. Related behavior has been reported in layered transition-metal chalcogenides such as $MoS_2$ and $MoSe_2$, where pressure-induced anisotropic compression is closely associated with enhanced interlayer coupling, dimensional crossover, and metallization [41,42]. In $FeNbTe_2$, the anomaly in $a/c$ may reflect a subtle change in the relative compression between the stacking direction and the in-plane framework. Such an anisotropic response could modify the interlayer coupling and local Fe–Te/Nb–Te hybridization, thereby affecting the bandwidth, magnetic exchange pathways, and carrier mobility. Importantly, these anomalies occur without any detectable symmetry change in the high-pressure XRD data. Thus, the present results do not support a conventional symmetry-changing structural transition as their origin.

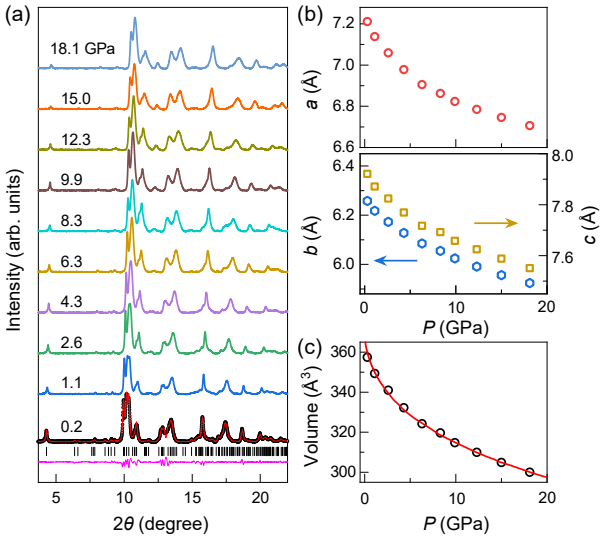


**Fig. 3.** (a) Room-temperature high-pressure synchrotron XRD patterns of pulverized $FeNbTe_2$ single crystals at selected pressures ($\lambda = 0.5426$ Å), together with Le Bail refinements. The open circles and the red line represent observed and calculated data, respectively. The vertical bars indicate Bragg peak position, and the violet lines show the difference between observed data and theoretical calculation. (b) Pressure dependences of the lattice parameters $a$, $b$, and $c$. (c) Pressure dependence of the unit-cell volume; the solid line is the Birch-Murnaghan equation of states fit.

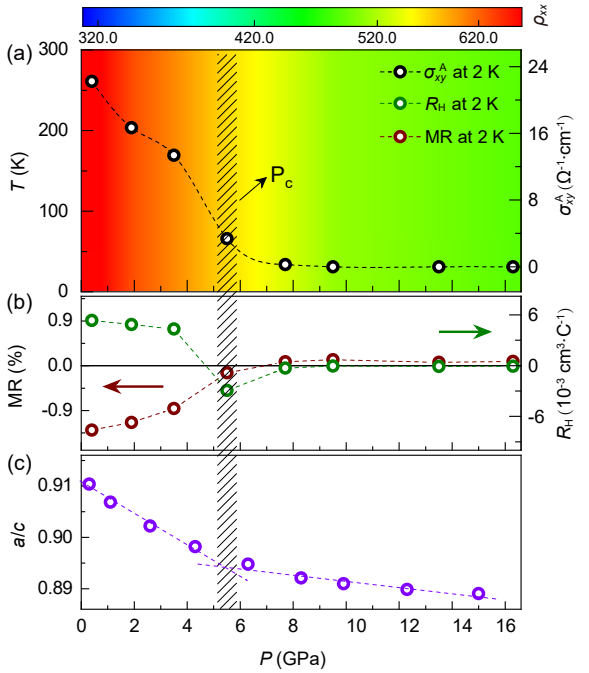


**Fig. 4.** (a) Contour plot of the resistivity as a function of temperature and pressure, overlaid with the pressure dependence of the anomalous Hall conductivity $\sigma_{xy}^{A}$ measured at 2 K. (b) Pressure dependences of the MR and Hall coefficient ($R_H$) measured at 2 K and 2 T. (c) Pressure dependence of the structural parameter ratio $a/c$.

To examine whether the transport anomalies are connected to changes in the electronic structure, we performed pressure-dependent first-principles band-structure calculations, as shown in Fig. S5 of the SM. The calculated bands exhibit pronounced pressure-induced changes near the Fermi level. In particular, a band inversion develops

along the $Y$–$T$ direction under compression, indicating a substantial reconstruction of the electronic structure. Concurrently, the electron pocket around the $Y$ point expands with increasing pressure. These features indicate that pressure modifies the electronic structure and enhances the electron-like contribution, providing a microscopic basis for the Hall-sign reversal and the accompanying suppression of the anomalous Hall response. Similar phenomena have also been discussed in several pressure-tuned systems, including $PtTe_2$, $CsV_3Sb_5$, $Ta_2PdSe_6$, and 6R-$TaS_2$ [43–48]. In these systems, transport anomalies are closely linked to pressure-driven changes in the electronic structure while the crystallographic framework remains preserved. In $FeNbTe_2$, the evolution of the Hall coefficient, anomalous Hall response, and $a/c$ ratio, together with the calculated band structure, points to a pressure-driven electronic reconstruction within the monoclinic phase. This electronic reconstruction naturally accounts for the marked reorganization of carrier transport and magnetic transport response near $P_c$.

## Conclusions

In summary, we have investigated the pressure evolution of monoclinic $FeNbTe_2$ through combined electrical transport, magnetoresistance, Hall effect, and synchrotron XRD measurements. A pronounced set of anomalies develops near the characteristic pressure $P_c \sim 5.5$ GPa, where the low-temperature resistive upturn is rapidly suppressed, the negative magnetoresistance and anomalous Hall response collapse, and the Hall coefficient reverses sign. Room-temperature high-pressure XRD shows that the monoclinic $P2_1/c$ structure remains intact over the investigated pressure range, although the $a/c$ ratio exhibits a weak anomaly near $P_c$. Together with pressure-dependent band-structure calculations, these results indicate a pressure-driven electronic reconstruction in monoclinic $FeNbTe_2$, accompanied by a marked modification of carrier transport and magnetic transport response within the preserved monoclinic framework. Our work establishes monoclinic $FeNbTe_2$ as a useful platform for studying pressure-tuned carrier balance, magnetic scattering, and anomalous transverse transport in layered tellurides.

## Data Availability

The data that support the findings of this article are not publicly available but are available from the authors upon reasonable request.

## Acknowledgments

This work was supported by the National Key R&D Program of China (Nos. 2024YFA1408102 and 2023YFA1406400), the National Natural Science Foundation of China (NSFC) (Nos. 12504051 and 12304175), and the Zhejiang Provincial Natural Science Foundation of China (No. LQN26A040013). The DFT calculations were performed on the supercomputers of HPC center and Advanced Computing Center at Hangzhou Normal University in China. The synchrotron XRD measurements were done at high performance Membrane protein crystallography beamline BL17UM of the Shanghai Synchrotron Radiation Facility (https://cstr.cn/31124.02.SSRF.BL17UM).

## References

[1] Nagaosa N, Sinova J, Onoda S, MacDonald A H, and Ong N P 2024 *Rev. Mod. Phys.* **82** 1539
[2] Xiao D, Chang M C, and Niu Q 2010 *Rev. Mod. Phys.* **82** 1959
[3] Nakatsuji S, Kiyohara N, and Higo T 2015 *Nature* **527** 212
[4] Liu E K, Sun Y, Kumar N, Muechler L, Sun A L, Jiao L, Yang S Y, Liu D F, Liang A J, Xu Q N, Kroder J, Süß V, Borrmann H, Shekhar C, Wang Z S, Xi C Y, Wang W H, Schnelle W, Wirth S, Chen Y L, Goennenwein S T B, and Felser C 2018 *Nat. Phys.* **14** 1125
[5] McIver J W, Schulte B, Stein F U, Matsuyama T, Jotzu G, Meier G, and Cavalleri A 2020 *Nat. Phys.* **16** 38
[6] Gonzalez Betancourt R D, Zubáč J, Gonzalez-Hernandez R, Geishendorf K, Šobáň Z, Springholz G, Olejník K, Šmejkal L, Sinova J, Jungwirth T, Goennenwein S T B, Thomas A, Reichlová H, Železný J, and Kriegner D 2023 *Phys. Rev. Lett.* **130** 036702
[7] Zhang P, Si K P, Wang X G, Zhao F F, Li B X, Wei J T, Yang Y H, Tang P Z, Liu Z, Wu K, and Gong Y J 2025 *Adv. Mater.* **37** e09261
[8] Zhou L J, Yan Z J, Rong H T, Zhao Y F, Xiao P, Lai L K, Xi Z Y, Wang K, Adhikari T, Tiwari G P, Lin Z, Manue P, Orlandi F, Khalyavin D, Grutter A J, Liu C X, Yan B H, and Chang C Z 2026 arXiv: 2602.09363 [cond-mat. mtrl-sci]
[9] Kirshenbaum K, Syers P S, Hope A P, Butch N P, Jeffries J R, Weir S T, Hamlin J J, Maple M B, Vohra Y K, and Paglione J 2013 *Phys. Rev. Lett.* **111** 087001
[10] Zhang J L, Guo C Y, Zhu X D, Ma L, Zheng G L, Wang Y Q, Pi L, Chen Y, Yuan H Q, and Tian M L 2017 *Phys. Rev. Lett.* **118** 206601
[11] Wang N N, Wang G, Shen X L, Hou J, Luo J, Ma X P, Yang H X, Shi L F, Dou J, Feng J, Yang J, Shi Y Q, Ren Z A, Ma H M, Yang P T, Liu Z Y, Liu Y, Zhang H, Dong X L, Wang Y X, Jiang K, Hu J P, Nagasaki S, Kitagawa K, Calder S, Yan J Q, Sun J P, Wang B S, Zhou R, Uwatoko Y, and Cheng J G 2024 *Nature* **634** 579
[12] Zhang M X, Pei C Y, Peng D, Du X, Hu W X, Cao Y T, Wang Q, Wu J F, Li Y D, Liu H Y, Wen C H P, Song J, Zhao Y, Li C H, Cao W Z, Zhu S H, Zhang Q, Yu N, Cheng P H, Zhang L L, Li Z W, Zhao J K, Chen Y L, Jin C Q, Guo H J, Wu C J, Yang F, Zeng Q S, Yan S C, Yang L X, and Qi Y P 2025 *Phys. Rev. X* **15** 021005
[13] Shi M Z, Peng D, Fan K B, Xing Z F, Yang S H, Wang Y Z, Li H P, Wu R Q, Du M, Ge B H, Zeng Z D, Zeng Q S, Ying J J, Wu T, and Chen X H 2025 *Nat. Phys.* **21** 1780
[14] Sun Z L, Peng K L, Cui J H, Zhu C S, Zhuo W Z, Wang Z Y, and Chen X H 2021 *Phys. Rev. B* **103** 085116
[15] Yu F H, Wen X K, Gui Z G, Wu T, Wang Z Y, Xiang Z J, Yin J J, and Chen X H 2022 *Chin. Phys. B* **31** 017405
[16] Scharf G, Guterding D, Hen B, Sarte P M, Ortiz B R, Rozenberg G Kh, Holder T, Wilson S D, and Jeschke H O 2025 *Phys. Rev. Res.* **7** 013127
[17] Li J, Badding M E, and DiSalvo F J 1992 *Inorg. Chem.* **31** 1050
[18] Zhang J H, Chen F, Li J, and O'connor C J 1997 *J. Appl. Phys.* **81** 5283
[19] Qi B T, Guo J J, Miao Y Q, Zhong M Z, Li B, Luo Z Y, Wang X G, Nie Y Z, Xia Q L, and Guo G H 2022 *Front. Phys.* **10** 851838
[20] Bai W, Hu Z Q, Wang S, Hua Y, Sun Z, Xiao C, and Xie Y 2019 *Adv. Mater.* **31** 1900246
[21] Wang D, Yang L, Hu Z, Wang F, Yang Y, Pan X K, Dong Z, Tian S J, Zhang L B, Han L, Jiang M J, Tang K Q, Dai F X, Zhang K, Lu W, Chen X S, Wang L, and Hu W D 2025 *Nat. Commun.* **16** 25
[22] Wu H L, Li S, Lyu Y, Guo Y C, Liu W H, Seop Oh J, Zhang Y C, Mo S K, dela Cruz C, Birgeneau R J, Taddei K M, Yi M, Yang L, and Lv B 2024 *Phys. Rev. B* **109** 174427
[23] Stepanova A V, Mironov A V, Bogach A V, Azarevich A N, Presniakov I A, Sobolev A V, Pankratov D A, Zayakhanov V A, Starchikov S S, Verchenko V Y, and Shevelkov A V 2024 *Chem. Commun.* **60** 5518
[24] Gao M H, Zhang Y, Sun S T, Yin C H, Yang Z K, Lv Y Y, Zhou J, Feng J H, Yao S H, Chen Y B, and Chen Y F 2025 *Phys. Rev. Res.* **7** 023219
[25] Yang H Y, Zhou Y H, Wang S Y, Wang J, Chen X L, Zhang L L, Xu C C, and Yang Z R 2023 *Phys. Rev. B* **107** L020503
[26] Prescher C and Prakapenka V B 2015 *High Press. Res.* **35** 223
[27] Hunter B A *Rietica-A Visual Rietveld Program* (International Union of Crystallography Commission on Powder Diffraction Newsletter, No. 20 Summer, 1998) http://www.rietica.org
[28] Mao H K, Xu J, and Bell P M 1986 *J. Geophys. Res.* **91** 4673
[29] Kresse G and Hafner J 1993 *Phys. Rev. B* **47** 558
[30] Kresse G and Joubert D 1999 *Phys. Rev. B* **59** 1758
[31] Perdew J P, Burke K, and Ernzerhof M 1996 *Phys. Rev. Lett.* **77** 3865
[32] Souza I, Marzari N, and Vanderbilt D 2001 *Phys. Rev. B* **65** 035109
[33] Zhi G X, Xu C, Wu S Q, Ning F, and Cao C 2022 *Comput. Phys. Commun.* **271** 108196
[34] Wu Q S, Zhang S N, Song H F, Troyer M, and Soluyanov A A 2018 *Comput. Phys. Commun.* **224** 405
[35] Chen Q, Tian Y X, Wang L, Niu C, Jiang W, Mao H N, Zhai Y, Jia Z, Jiang Y, and Xia K 2026 *Nat. Commun.* **17** 1736
[36] Tateiwa N and Haga Y 2009 *Rev. Sci. Instrum.* **80** 123901
[37] Muroi M, Street R, McCormick P G, and Amighian J 2001 *Phys. Rev. B* **63** 184414
[38] Gantmakher V F, Levinson Y B, Grinberg A A, and Luryi S 1988 *Phys.*

*Today* **41** 84
[39] Shen B, Du F, Breitner F, Ginga V A, Uykur E, Tsirlin A A, and Gegenwart P 2025 arXiv: 2503.09524 [cond-mat. str-el]
[40] Birch F 1947 *Phys. Rev.* **71** 809
[41] Guo H, Yang T, Tao P, Wang Y, and Zhang Z 2013 *J. Appl. Phys.* **113** 013709
[42] Zhao Z, Zhang H. Yuan H, Wang S, Lin Y, Zeng Q, Xu G, Liu Z, Solanki G K, Patel K D, Hwang H Y, and Mao W L 2015 *Nat. Commun.* **6** 7312
[43] Liu F L, Li J H, Zhang K N, Peng S, Huang H Q, Yan M Z, Li N N, Zhang Q, Guo S H, Lü X J, Cai P, Yin L F, Zhou S Y, Duan W H, Shen J, and Yang W G 2018 *Sci. China Phys. Mech. Astron.* **62** 48211
[44] Zhang Z Y, Chen Z, Zhou Y, Yuan Y F, Wang S Y, Wang J, Yang H Y, An C, Zhang L L, Zhu X D, Zhou Y H, Chen X L, Zhou J H, and Yang Z R 2021 *Phys. Rev. B* **103** 224513
[45] Yu F H, Zhu X D, Wen X K, Gui Z G, Li Z Y, Han Y L, Wu T, Wang Z Y, Xiang Z J, Qiao Z H, Ying J J, and Chen X H 2022 *Phys. Rev. Lett.* **128** 077001
[46] Wen X K, Li Z Y, Gui Z G, Zhang Y Q, Li Y K, Li Y J, Liu Q Y, Xiang Z J, Cai J Q, Xi C Y, Zhang J L, Qiao Z H, Ying J J, and Chen X H 2026 *Phys. Rev. Res.* **8** 013197
[47] Yang H Y, Zhou Y H, Li L Y, Chen Z, Zhang Z Z, Wang S Y, Wang J, Chen X L, An C, Zhou Y, Zhang M, Zhang R R, Zhu X D, Zhang L L, Yang X P, and Yang Z R 2022 *Phys. Rev. Mater.* **6** 084803
[48] Lv X D, Song H, Chen K, Liu S R, Huang Y P, Fang Y Q, Shen Z X, and Cui T 2024 *Sci. China Phys. Mech. Astron.* **67** 128211